Lipid Headgroup Spacing and Peptide Penetration, but Not Peptide Oligomerization, Modulate Peptide-Induced Fusion†

Eve-Isabelle Pécheur,*,‡ Josette Sainte-Marie,§ Alain Bienvenüe,§ and Dick Hoekstra*,‡

Department of Physiological Chemistry, University of Groningen, Antonius Deusinglaan 1, 9713 AV Groningen, The Netherlands, and UMR 5539 CNRS, Dynamique Moléculaire des Interactions Membranaires, Dépt Biologie Santé, cc 107, Université Montpellier II, Place Eugène Bataillon, F-34095 Montpellier Cedex 5, France

Received June 12, 1998; Revised Manuscript Received October 15, 1998

ABSTRACT: In this study, the mechanism by which an amphipathic negatively charged peptide consisting of 11 amino acids (WAE) induces fusion of liposomal phosphatidylcholine membranes is investigated. WAE-induced fusion, which only occurs when the peptide is covalently attached to the bilayer, shows a highly remarkable dependence on naturally occurring phosphatidylcholine species. The initial rate of fusion increased in the order 1-palmitoyl 2-arachidonoyl PC (PAPC) > 1-palmitoyl 2-oleoyl PC (POPC) > 1-stearoyl 2-oleoyl PC (SOPC) > dioleoyl PC (DOPC) > egg yolk PC. Interestingly, the susceptibility of the various PC species toward WAE-induced fusion matched a similar order of increase in intrinsic lipid headgroup spacing of the target membrane. The degree of spacing, in turn, was found to be related to the extent by which the fluorescence quantum yield of the Trp residue increased, which occurred upon the interaction of WAE with target membranes. Therefore, these results demonstrate an enhanced ability for WAE to engage in hydrophobic interactions when headgroup spacing increases. Thus, this latter parameter most likely regulates the degree of penetration of WAE into the target membrane. Apart from penetrating, WAE oligomerizes at the site of fusion as revealed by monitoring the self-quenching of the fluorescently derivatized lipid anchor to which WAE is attached. Clustering appears specifically related to the process of membrane fusion and *not* membrane aggregation. This is indicated by the fact that fusion and clustering, but not aggregation, display the same strict temperature dependence. However, evidence is presented indicating that clustering is an accompanying event rather than a prerequisite for fusion. The notion that various biologically relevant fusion phenomena are accompanied by protein clustering and the specific PC-species-dependent regulation of membrane fusion emphasize the biological significance of the peptide in serving as a model for investigating mechanisms of protein-induced fusion.

Membrane fusion is of pivotal significance in the biological life of a cell. It is involved in intracellular processes such as endo- and exocytosis (*1*), as well as in intercellular processes such as cell−cell interactions, including myoblast fusion (*1*) and sperm−egg fusion (*2*). Of particular interest is also the mechanism of cellular infection by enveloped viruses, which similarly involves distinct membrane fusion steps (*3*). A common feature in cellular and viral fusion phenomena is the involvement of specific fusion proteins, which contain a so-called "fusion peptide" in their sequence. In many viral fusion proteins, these peptides are short segments (ca. 20 amino acids) composed of relatively hydrophobic amino acids. They are thought to penetrate into the target membrane and cause fusion through the destabilization they induce. While (membrane-associated) fusion proteins play a crucial role in mediating fusion (*1*), the lipid composition of the fusing membranes appears of relevance as well. For example, fusion of Semliki Forest virus (*4*), Sendai virus (*5*), and vesicular stomatitis virus (*6*) with their target cells was shown to depend on the presence of cholesterol in the target membrane. Similarly, fusion of reticulocyte endocytic vesicles with model membranes (*7*) and that of endoplasmic reticulum-derived vesicles with the Golgi (*8*) is strongly enhanced by the presence of unsaturated PE[1] in the target membrane. Due to their cone-shaped molecular structure (for a review see ref *9*), nonbilayer lipids such as cholesterol and unsaturated PE are able to promote the bilayer-to-nonbilayer transition, a condition that will obviously facilitate membrane merging.

† We acknowledge the financial support obtained from the European Commission, Contract No. BIO4-CT97-2191. E.-I.P. is a recipient of a fellowship from the Ministère Français des Affaires Etrangères, bourse Lavoisier No. 6033 STR/FE.

* Corresponding authors. E-mail: e.pecheur-huet@med.rug.nl. Fax: (31) 50-363-2728. E-mail: dhoekstra@med.rug.nl.

‡ University of Groningen.

§ Université Montpellier II.

[1] Abbreviations: EYPC, egg yolk phosphatidylcholine; POPC, 1-palmitoyl-2-oleoyl phosphatidylcholine; SOPC, 1-stearoyl-2-oleoyl phosphatidylcholine; DOPC, dioleoyl phosphatidylcholine; PAPC, 1-palmitoyl-2-arachidonoyl phosphatidylcholine; DPPC, L-α-dipalmitoylphosphatidylcholine; DPPE, L-α-dipalmitoylphosphatidylethanolamine; LPC, *lyso*-1-oleoyl-*sn*-3-phosphatidylcholine; chol, cholesterol; PE-PDP, *N*-succinimidyl 3-(2-pyridyldithio)propionate-derivatized DPPE; PElys, lysine coupled to L-α-dipalmitoylphosphatidylethanolamine; RET, resonance energy transfer; BSA, bovine serum albumin; *N*-NBD-PE, *N*-(7-nitro-2,1,3-benzoxadiazol-4-yl)phosphatidylethanolamine; *N*-Rh-PE, *N*-(Lissamine rhodamine B sulfonyl)dihexadecanoyl-*sn*-glycero-3-phosphoethanolamine; C_{12}-NBD-PE, 1-oleoyl-2-[12-(7-nitro-2,1,3-benzoxadiazol-4-yl)amino]dodecanoyl phosphatidylethanolamine; dansylPE, *N*-(5-(dimethylamino)naphthalenyl-1-sulfonyl)-1,2-dipalmitoyl phosphatidylethanolamine.

10.1021/bi981389u CCC: $18.00
Published on Web 12/08/1998

Concerning lamellar lipids such as phosphatidylcholine, one of the major lipid species of biological membranes, very little is known as to their ability to modulate membrane fusion except for the fact that their relatively strongly hydrated headgroup inhibits membrane fusion in model systems (*1, 3*). However, the extent to which each of the various PC species, as defined by differences in fatty acid chain composition, could modulate fusion of PC-containing membranes is obscure.

The mechanism underlying protein-induced fusion is thought to involve a penetration (at least partially) of the fusion-peptide into the target membrane (*10, 11*). Interestingly, some recent work on the role of PC in affecting protein kinase C activity suggested a correlation between its activity and membrane penetration of the enzyme, the latter being dictated by the (un)saturation of the PC acyl chains (*12*). This feature may thus bear an analogy to requirements of peptide penetration as an inherent part of a membrane fusion mechanism, implying that PC species could regulate membrane fusion susceptibility.

As a novel model for fusion induced by a membrane-anchored protein, we have recently synthesized a short peptide, consisting of only 11 amino acids, abbreviated as WAE. We have previously demonstrated that the peptide triggers membrane fusion, provided that it is anchored to the liposomal surface, thus closely matching features of *membrane-associated* viral fusion proteins (*13*). To examine the mechanism of WAE-induced fusion and to verify the relevance of parameters in fusion as described above, the effect of PC species on the fusion process was studied in detail. Evidence is presented which demonstrates the existence of a relationship between lipid headgroup spacing and fusion. Thus increasing headgroup spacing represents a parameter which relates to the relative ease of penetration of the peptide into the target membrane and its ensuing ability to engage in hydrophobic interactions. Another novel feature in modeling peptide-induced fusion entails the observation that peptide oligomerization occurs during the fusion event but *not* upon aggregation. Most interestingly, this clustering phenomenon was found to be an accompanying event rather than a prerequisite for fusion. The data emphasize the validity of the WAE peptide as a convenient model to study the mechanism of membrane fusion, in a biologically relevant context.

MATERIALS AND METHODS

Chemicals. Egg yolk PC,[1] 1-palmitoyl-2-oleoyl PC (POPC), 1-stearoyl-2-oleoyl PC (SOPC), L-α-dipalmitoylphosphatidylcholine (DPPC), L-α-dipalmitoyl-phosphatidylethanolamine (DPPE), cholesterol (chol), bovine serum albumin (BSA, essentially fatty acid free), *lyso*-1-oleoyl-*sn*-3-phosphatidylcholine (LPC), 1-monooleoyl-*rac*-glycerol (monoolein), and polyoxyethylene glycol 8000 (PEG-8000) were obtained from Sigma. [^{14}C]-lyso-1-palmitoyl-*sn*-3-phosphatidylcholine ([^{14}C]-LPPC) was purchased from Amersham. DOPC, POPC, PAPC, and 1-oleoyl 2-[12-(7-nitro-2,1,3-benzoxadiazol-4-yl)amino]dodecanoyl phosphatidylethanolamine (C_{12}-NBD-PE) were from Avanti Polar Lipids. *N*-succinimidyl-3-(2-pyridyldithio)propionate (SPDP)-derivatized DPPE (PE-PDP) and C_{12}-NBD-PE (C_{12}-NBD-PE-PDP) were synthesized as described earlier (*14*). Lysine-derivatized PE (PElys) and C_{12}-NBD-PE (C_{12}-NBD-PElys) were prepared by covalent coupling of L-Lys to DPPE or C_{12}-NBD-PE, as described by Puyal et al. (*15*). The fluorescent lipid analogues *N*-(7-nitro-2,1,3-benzoxadiazol-4-yl) phosphatidylethanolamine (*N*-NBD-PE), *N*-(Lissamine rhodamine B sulfonyl) phosphatidylethanolamine (*N*-Rh-PE), and *N*-(5-(dimethylamino)-naphthalene-1-sulfonyl)-1,2-dipalmitoyl phosphatidylethanolamine (dansylPE) were purchased from Molecular Probes. All other reagents were of analytical grade.

The polyunsaturated PC species were handled so as to minimize oxidation. Vesicles prepared from those lipids were kept at 4 °C in the dark and used within a few hours after preparation. No oxidation products were detected, as monitored by thin-layer chromatography and conjugated dienes tests (*16, 17*).

Preparation of Liposomes. All liposomes were prepared by sonication followed by extrusion, as described (*13*). The liposomes were sized to a diameter of approximately 150 nm, as verified by electron microscopy and dynamic light scattering. Positively charged liposomes were composed of PC (various species)/chol/PElys (11:6:3). The 11-mer peptide "N-Trp-Ala-Glu-Ser-Leu-Gly-Glu-Ala-Leu-Glu-Cys" (WAE) was synthesized and purified to more than 95% purity by Synt:em SA (Nîmes, France). The peptide was then coupled to liposomes (referred to as donor liposomes throughout the paper) composed of egg yolk PC (EYPC)/chol/PE-PDP (3.5:1.5:0.25, unless otherwise stated), and to monitor fusion by a lipid mixing assay (see below), 1 mol % each of *N*-NBD-PE and *N*-Rh-PE (*13*) was used. Uncoupled peptide was removed by filtering the liposome sample through a Sephadex G-25 gel (PD-10 column, Pharmacia). Coupling is accomplished via disulfide bonding between the peptide's terminal Cys residue and PE-PDP (for details see ref *13*). The coupling efficiency was evaluated spectrophotometrically at 343 nm, by monitoring the release of 2-mercaptopyridine. The lipid phosphorus content was measured by Bartlett's method (*18*), and the cholesterol content by the ferric chloride method (*19*).

Resonance Energy Transfer (RET) Assay for Lipid Mixing. Lipid mixing of vesicles, as a measure of fusion, was assayed as described by Struck et al. (*20*). Peptide-coupled liposomes containing 1 mol % each of *N*-NBD-PE and *N*-Rh-PE were added to a suspension of PElys-containing vesicles in 10 mM Tris, 150 mM NaCl, pH 7.4, at a lipid molar ratio of 1:6 (total lipid concentration 70 μM). The increase in NBD fluorescence was monitored as a function of time in an SLM SPF-500C spectrofluorimeter ($\lambda_{exc} = 460$ nm, $\lambda_{em} = 534$ nm) under continuous stirring. The temperature was controlled with a thermostated circulating water bath. The excitation and emission band slits were 2 nm. Peak absorbance of samples was kept below 0.1 to reduce inner filter effects. For calibration, 0% taken as the intrinsic fluorescence intensity of NBD/Rh-labeled liposomes and 100% fluorescence was obtained after addition of 0.2% Triton X-100 (final concentration), corrected for detergent-induced quenching of NBD fluorescence. As a proper reflection of the fusion event in terms of rate and extent (cf. ref *13*), fusion is expressed as the initial rate of fusion, calculated from the tangent drawn to the steepest part of the fluorescence tracing.

Determination of Lipid Headgroup Spacing. Lipid headgroup spacing at the level of target liposomes was determined by using dansylPE. The lipid analogue was incorporated into

liposomes during their preparation (probe/lipid concentration ratio 1:100). After a 10 min equilibration period at 30 °C, the fluorescence intensity was measured (λ_{exc} = 340 nm, λ_{em} = 528 nm) in buffers made up in D_2O and H_2O, respectively, and the ratio was calculated as described (*21*). Note that all measurements were performed in the absence of the peptide-coupled vesicles.

Fluorescence Assay for Monitoring Peptide Clustering. WAE peptide was coupled to liposomes composed of EYPC/chol/C_{12}-NBD-PE-PDP, and the assessment of the segregation of WAE was determined by monitoring self-quenching of NBD fluorescence (*22*). Consistent with previous observations on long-chain i.e., C_{12}-derivatized lipid analogues (*23*, *24*), C_{12}-NBD-PE-PDP remains firmly associated with the donor membrane, without monomeric transfer to target vesicles during the time course of the experiment (not shown). Note that for a concentration of 5 mol %, a self-quenching of ca. 30% is obtained as measured by determining the fluorescence before and after addition of Triton X-100. This extent of self-quenching is entirely consistent with a lateral distribution as monomers in the donor membranes, as previously reported for various phospholipid analogues (*22*). The coupling efficiency of the added *peptide fraction* is approximately 10−20% (*13*), implying that, at a density of 5 mol % C_{12}-NBD-PE-PDP and a peptide/PE-PDP ratio of 5:1, at least half of the fluorescent-derivatized peptide anchor contains coupled peptide. At such a density, lateral changes in the density of the analogue, as reflected by a change in fluorescence self-quenching, will be readily detectable, analogously as previously reported (*22*).

The change in the fluorescence intensity was examined after a 2 min equilibration of the fluorescently labeled vesicles in buffer at the desired temperature.

The segregation of PElys in the target membranes was assessed in a similar manner, by monitoring self-quenching of C_{12}-NBD-PElys (see above).

Tryptophan Fluorescence Measurements. Emission spectra of the peptide-coupled liposomes suspended in 10 mM Tris, 150 mM NaCl, pH 7.4, were recorded as a function of temperature or PC species between 300 and 400 nm at λ_{exc} = 280 nm, in the absence or presence of target vesicles. The spectra were corrected for the vesicle blank (scatter) and for the dilution caused by the liposome addition. Trp fluorescence measurements were done in the absence and presence of iodide, which acts as an aqueous collisional quencher of Trp, as described earlier (*25*).

RESULTS

WAE-Induced Fusion Displays a Distinct Threshold Temperature and Depends on the PC Species in the Target Membranes. Previously, we demonstrated that WAE induces membrane fusion, provided that the peptide is coupled to the membrane surface (*13*, *25*). Also, lipid mixing reliably reflects the occurrence of membrane fusion, as verified by contents mixing which proceeds in the absence of any significant leakage of vesicle contents. As will be indicated below, these features also hold for the fusion of WAE-coupled vesicles and the various target vesicles used in the present study. For convenience, lipid mixing is therefore applied to monitor membrane merging, referred to as "fusion" throughout this work.

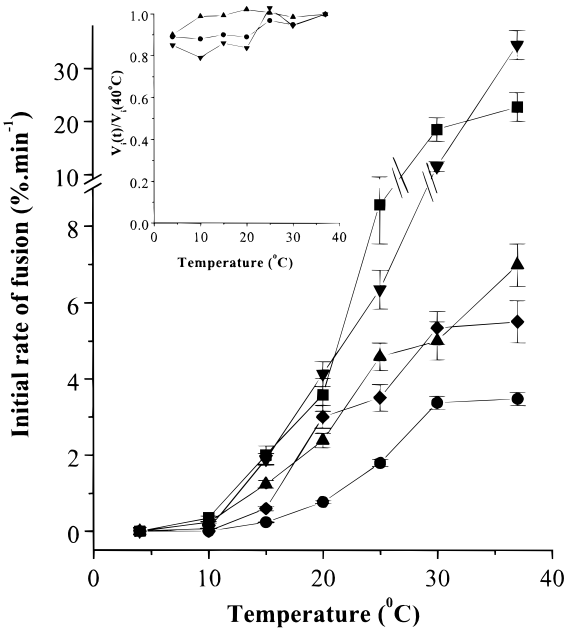

FIGURE 1: Effect of temperature on the fusion and aggregation between WAE-coupled liposomes and target vesicles of various PC species. WAE-coupled liposomes, composed of EYPC/chol (3.5:1.5; see Materials and Methods) and labeled with 1 mol % each of *N*-NBD-PE and *N*-Rh-PE, were added to PC/chol/PElys (11:6:3) target vesicles containing as PC species EYPC (●), DOPC (▲), PAPC (■), POPC (▼), and SOPC (◆), at the desired temperature in a lipid molar ratio 1:6 (total lipid concentration, 70 μM). The buffer was 10 mM Tris, 150 mM NaCl, pH 7.4. Lipid mixing was followed by monitoring the increase in *N*-NBD-PE fluorescence. The initial fusion rates were calculated from the tangents drawn to the steepest part of the curves and plotted as a function of temperature. Inset: aggregation was followed by measuring the turbidity of the suspensions at 500 nm as a function of temperature. The initial aggregation rates [$V_i(t)$] at a given temperature, *t*, were calculated from the tangents drawn to the steepest part of the curves and normalized to the initial rate obtained at 40 °C [V_i(40 °C)]. Symbols are similar to those for lipid mixing.

Upon addition of EYPC (and cholesterol)-containing target vesicles to WAE-coupled liposomes, the onset of fusion, as detected by lipid mixing, shows a threshold temperature which is centered around 15 °C (Figure 1, circles). Upon further increase of the incubation temperature (20−37 °C), the initial rate of fusion rapidly increases, with a maximal rate of fusion reached at approximately 30 °C. EYPC contains a mixture of saturated and unsaturated fatty acid species [i.e. POPC (37%), SOPC (10%), DOPC (7%), and PAPC (3%) (*26*)], which may exert differential effects on PC/cholesterol interaction. Thus, such features could in principle selectively modulate WAE's ability to trigger membrane fusion. To examine this possibility, we investigated the effect of defined PC species on WAE-induced mixing of lipids and internal contents. Thus, target liposomes (PC/chol/PElys, 11:6:3) were prepared in which the PC species was either dioleoylphosphatidylcholine (DOPC), 1-palmitoyl-2-arachidonoylphosphatidylcholine (PAPC), 1-palmitoyl-2-oleoylphosphatidylcholine (POPC), or 1-stearoyl-2-oleoylphosphatidylcholine (SOPC). The WAE-containing vesicles consisted in each case of EYPC/chol (3.5:1.5). As shown in Figure 1, the temperature dependence of fusion for each system was very reminiscent of that of the EYPC target vesicles, displaying threshold temperatures between 10 and 15 °C. Interestingly, however, the nature of the PC

species notably affects the kinetics of WAE-induced fusion. Thus, relative to EYPC-containing target vesicles, higher initial rates (and extents, data not shown) of fusion were obtained for bilayers composed of a single PC species, fusion increasing according to the following general trend: PAPC > POPC > SOPC ≈ DOPC > EYPC. As previously reported (see refs *13* and *25* and above), the observed rates of lipid dilution reported for the various mixtures reflected the occurrence of genuine fusion. Thus when monitored by a contents mixing assay, none of the examined vesicle systems showed significant leakage of contents (not shown). For example, in the case of POPC/chol vesicles, the overall kinetics of lipid mixing (initial rate 11.5%·min^{-1} at 30 °C, extent 12% after 5 min.) and contents mixing (10.5%·min^{-1}, extent 10% after 5 min) were very similar (cf. ref *13*). For PAPC- and DOPC-containing vesicles, the initial rates of lipid- and contents-mixing (at 30 °C) were 19 vs 20%·min^{-1} and 8.7 vs 6.5%·min^{-1}, respectively; after 5 min the extents of lipid mixing and contents mixing were respectively 16 vs 19% in the case of PAPC-containing vesicles and 8.5 vs 7% in the case of DOPC-containing vesicles. Such features are thus entirely consistent with our previous observation on WAE-induced fusion of EYPC vesicles.

Finally, it should be emphasized that, for all PC species tested, the fusion step as such, and not aggregation, showed the particular dependence on temperature. Thus, as shown in Figure 1 (inset), the rates of aggregation remained fairly constant over the entire temperature range. Hence, these data demonstrate that temperature interferes with the peptide's fusion function rather than its aggregation capacity. The purpose of the experiments in the next paragraph was to investigate structural temperature-dependent parameters that apparently could control peptide-induced fusion.

Clustering of WAE is Concomitant to Peptide-Induced Fusion. The onset of fusion, which occurs around 10−15 °C irrespective of the PC species that was incorporated into the various lipid vesicles, does not coincide with the gel-to-liquid crystalline phase transition temperature (T_c) of the various target membranes. For each PC species, this transition occurs well below 0 °C. Rather, the next experiments were inspired by a reminiscence of the temperature dependence of WAE-induced fusion with fusion induced by viral proteins. In the latter system, it has been previously reported that virus attachment is fairly temperature-independent, in contrast to virus fusion which shows a very similar temperature dependence as WAE-induced fusion (*27*). In fact, in several viral systems, a relationship between the mobility of viral fusion proteins and membrane fusion activity has been demonstrated (*28, 29*).

To examine the role of mobility constraints, the peptide was coupled through PE-PDP (molar lipid ratio 0.25) to liposomes composed of either DOPC/chol (3.5:1.5) or EYPC/chol (3.5:1.5). Their fusion behavior versus EYPC or DOPC-containing target vesicles (overall composition PC/chol/PElys, 11:6:3) was then evaluated. Figure 2 shows that, irrespective of whether the peptide was coupled to a DOPC- or EYPC-containing lipid matrix, the initial rates of WAE-induced fusion as a function of temperature are essentially similar when, in both cases, DOPC vesicles acted as the target membrane (□, ■). By contrast, when the target membrane consisted of EYPC (○, ●), fusion is largely impaired, although less effectively when the peptide was

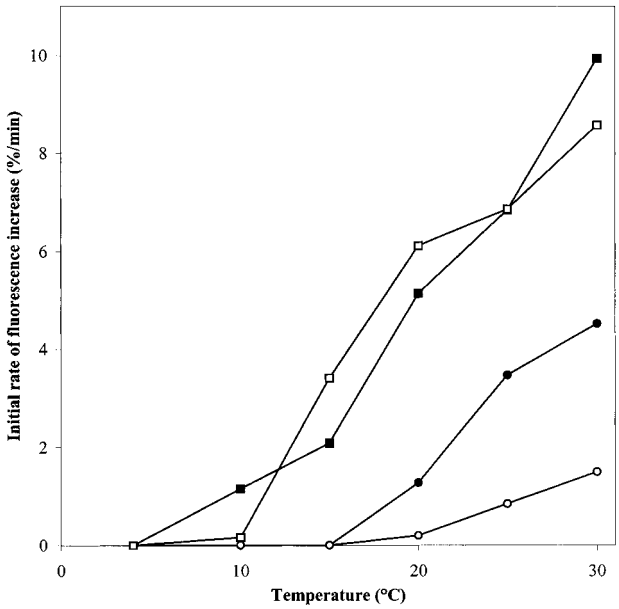

FIGURE 2: Influence of the lipid composition of WAE-coupled liposomes on their fusion activity with various target vesicles. WAE-coupled liposomes labeled with 1 mol % each of *N*-NBD-PE and *N*-Rh-PE and composed of either EYPC/chol (open symbols) or DOPC/chol (closed symbols) were added to a suspension of target vesicles, preequilibrated at the indicated temperatures, consisting of EYPC/chol (circles) or DOPC/chol (squares), in 10 mM Tris, 150 mM NaCl, pH 7.4. The rate of lipid mixing was monitored as described, and the initial rate was calculated and plotted as a function of temperature. Experimental conditions are identical to those in Figure 1.

coupled to the DOPC-containing lipid matrix. These observations thus demonstrate that the fusion process is also driven by distinct features displayed by the "donor" membrane to which the peptide is coupled.

Possibly, such features could be related to the lateral dynamics of the coupled peptide in the donor membrane. To monitor such dynamic changes, the peptide was covalently coupled to SPDP-derivatized C_{12}-NBD-labeled PE (see Materials and Methods). This approach will allow changes in the lateral distribution of WAE to be revealed as a change in NBD-fluorescence, as its intensity is dependent on its surface density (*22*). Thus, peptide-coupled EYPC bilayers were incubated with PElys-containing target vesicles at various conditions and the NBD-fluorescence was monitored as a function of time. The results, shown in Figure 3, demonstrate that the NBD-fluorescence decreases (quenches) at conditions that result in membrane fusion (a, b, and d), whereas self-quenching is *not* observed at conditions where fusion does not occur (c). Furthermore, the efficiency (i.e. the rate and extent) of fluorescence self-quenching increases when the efficiency of fusion increases (a > b > d). Control experiments revealed that neither in the absence of target vesicles or with peptide-devoid C_{12}-NBD-PE-PDP labeled donor vesicles nor upon addition of exogenous peptide did NBD fluorescence quenching occur (cf c in Figure 3). Also temperature by itself does not modify the lateral distribution of the C_{12}-NBD-PE-PDP-coupled peptide, since the degree of self-quenching, calculated after the addition of Triton X-100 to the sample, remains constant (around 33%) in the absence of target vesicles over the whole temperature range tested (see also ref *22*). It should be noted that, in this experiment, the C_{12}-NBD-PE-PDP does not interfere with

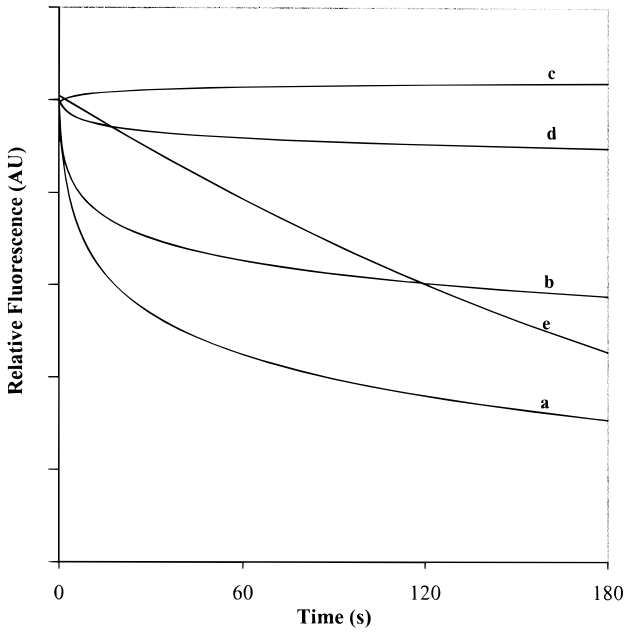

FIGURE 3: Kinetics of peptide clustering in EYPC/chol vesicles as a function of temperature and lipid composition of the target vesicles and kinetics of PElys clustering. WAE was coupled to EYPC/chol liposomes via PE-PDP, labeled in its acyl chain with the NBD fluorophore (C_{12}-NBD-PE-PDP). At time 0, target vesicles consisting of either DOPC/PElys (curves a−c) or EYPC/PElys (curve d) were added to a suspension of fluorescently labeled WAE-coupled liposomes. Recordings of NBD fluorescence quenching (expressed as arbitrary units of fluorescence) were made at 30 °C (a and d), 15 °C (b), or 6 °C (c). For PElys clustering, C_{12}-NBD-PElys was synthesized (see Materials and Methods) and incorporated into EYPC/chol target vesicles. At time 0, WAE-coupled liposomes were added to a suspension of these fluorescent vesicles, and a recording of NBD fluorescence quenching was made at 30 °C (curve e).

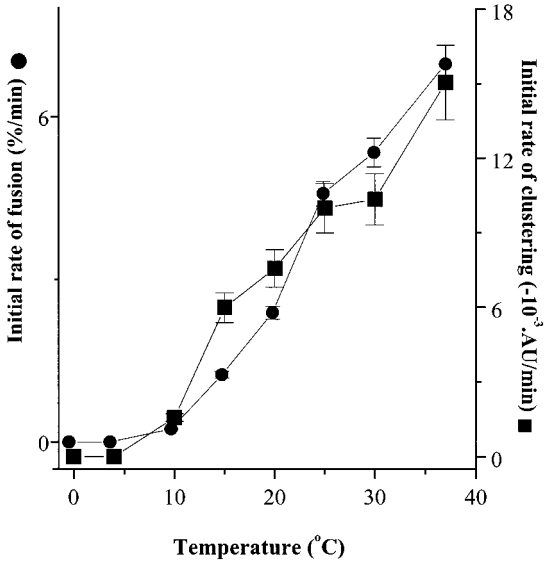

FIGURE 4: Clustering and fusion behavior of WAE as a function of temperature. WAE-coupled liposomes were added to a suspension of DOPC-containing target vesicles, preequilibrated at the indicated temperatures in 10 mM Tris, 150 mM NaCl, pH 7.4. For clustering experiments, WAE (■) was coupled to liposomes through C_{12}-NBD-PE-PDP, and the measurement was performed as described in the Materials and Methods section. The initial rate of clustering was calculated from the tangent drawn to the steepest part of the fluorescence tracing. For fusion experiments, WAE-coupled liposomes (●) were labeled with 1 mol % each of *N*-NBD-PE and *N*-Rh-PE; experimental conditions are identical to those in Figure 1. Results are expressed as mean ±SD of three different liposome preparations, in duplicate.

the kinetics of aggregation nor fusion. These latter were determined by an assay based upon RET between *N*-Rh-PE and the acyl chain-labeled lipid derivative. Although less sensitive, the kinetics obtained were similar to those observed in the lipid mixing in which *N*-Rh-PE and *N*-NBD-PE are employed (not shown).

To allow vesicle aggregation to occur, the target vesicles contain PElys, acting as an (electrostatic) acceptor for the negatively charged WAE. The next obvious question was whether peptide clustering under fusogenic conditions was accompanied by a concomitant clustering of PElys molecules. To examine this issue, C_{12}-NBD-PElys was synthesized and incorporated in place of its nonfluorescent counterpart into target vesicles. A segregation of PElys molecules was observed upon addition of peptide-coupled liposomes (curve e, Figure 3). Most importantly, clustering of PElys did not occur in the presence of free (nonfusogenic) peptide in solution nor at low temperature, i.e., conditions where WAE-mediated aggregation via interaction with PElys does occur but not fusion. Additional support for a fusion- rather than a vesicle aggregation-related oligomerization of WAE was obtained when a more systematic comparison was made between temperature-dependent fusion and clustering. As shown in Figure 4, the onset of peptide clustering with target DOPC vesicles shows a similar threshold temperature centered around 15 °C as the onset of fusion (Figure 4, squares vs circles). Furthermore, with increasing temperature, a commensurate increase in the rate of fusion and clustering is apparent. Importantly, as shown above (inset to Figure 1), aggregation remains unaffected by temperature over the range tested. To further substantiate our findings of a potential relationship between WAE clustering and fusion, peptide-coupled vesicles were prepared which differed in WAE density. It was anticipated that such a parameter would affect the rate of clustering and, if related, also that of fusion. Thus, the kinetics of NBD-fluorescence self-quenching and those of fusion were monitored, using liposomes containing 0.5, 2, and 5 mol % of SPDP-derivatized PE (corresponding to WAE coupling efficiencies of 2, 8, and 18%, respectively—see Materials and Methods). As shown in Figure 5, the peptide's density has a similar effect on both oligomerization and fusion events, the efficiency of fluorescence self-quenching, *and* of fusion decreasing when the density of the peptide at the surface of donor liposomes decreases.

Taken together, these results indicate that peptide's oligomerization properties are closely related to the peptide's ability to induce fusion, the kinetics of clustering following the same trend as the kinetics of fusion. Also, at a given temperature, clustering of WAE appears to be related to the fusion susceptibility of the target membranes (compare curves a for DOPC and d for EYPC, Figure 3). Importantly, the evidence which excludes aggregation as the driving force for WAE clustering (via a WAE−PElys interaction) is particularly strengthened by the observation that clustering is absent at conditions where aggregation occurs but not fusion.

However, the sequence of events leading to membrane merging still remains unclear, and the following experiments were designed to answer this question: is peptide oligomerization a prerequisite or an accompanying event of fusion?

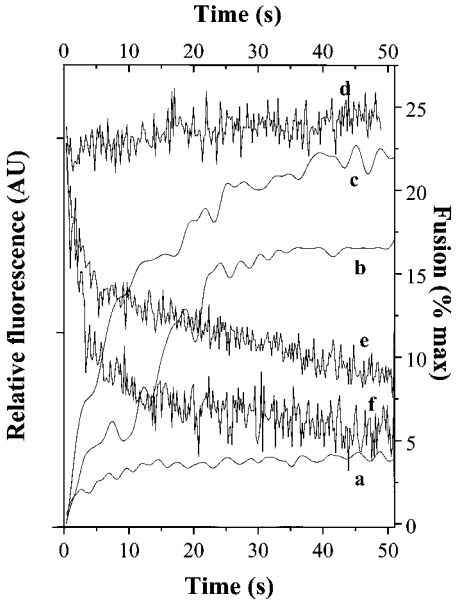

FIGURE 5: Influence of the peptide density on clustering and fusion. Fusion (curves a−c) and clustering (curves d−f) experiments were performed as described in the legend to Figure 4, with PE-PDP contents of 0.5 mol % (a and d), 2 mol % (b and e), and 5 mol % (c and f). The relative fluorescence of NBD, as a measure of clustering, was calculated from the equation $F/(F_0 - F_{min})$, in which F, F_0, and F_{min} denote the fluorescence at time t, the initial fluorescence of C_{12}-NBD-PE-PDP-containing liposomes (at various densities), and the intrinsic fluorescence of peptide−liposomes composed only of C_{12}-NBD-PE-PDP, respectively. Other experimental details are given in Materials and Methods.

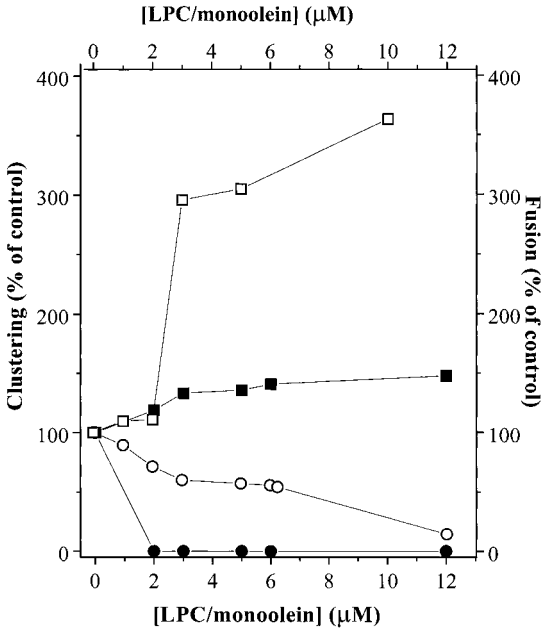

FIGURE 6: Effects of exogenously added lysoPC and monoolein on WAE clustering and WAE-induced lipid mixing. DOPC-containing target liposomes were incubated with increasing concentrations of LPC (○, ●) or monoolein (□, ■) for 3 min at 37 °C, and WAE-coupled fluorescent liposomes (C_{12}-NBD-PE-PDP, closed symbols, and *N*-NBD-PE/*N*-Rh-PE, open symbols) were added. The total lipid concentration was 70 μM, and LPC and monoolein were present at concentrations well below the lytic threshold (see text). Results are the mean of two different experiments, and SEM was within 5%.

Peptide Clustering Is Not a Prerequisite for Peptide-Induced Fusion. Previously, we demonstrated that lysophosphatidylcholine (LPC) and monoolein strongly inhibits or stimulates, respectively, WAE-induced fusion (*13*). It was therefore of interest to examine whether these compounds affected WAE clustering in a similar manner.

a. Effect of Lysophosphatidylcholine. In a first series of experiments, LPC (from an aqueous stock solution in buffer) was preincubated for 3 min with the PElys target vesicles. Subsequently, peptide-coupled vesicles were added and NBD-fluorescence dequenching (fusion) or self-quenching (clustering) was monitored, in separate experiments, as a function of time. As shown in Figure 6 (open circles), under conditions where fusion is still apparent (up to 6 μM LPC), peptide oligomerization (filled circles) is totally abolished. Note that a direct effect of LPC on the peptide molecule itself can be excluded, since (i) the kinetics and extent of aggregation are not affected by the presence of lysoPC, even at concentrations where fusion is completely abolished (12 μM LPC, Figure 6; see also *13*), and (ii) peptide-induced fusion and peptide clustering are similarly affected after preincubating LPC with either target or peptide-coupled vesicles (data not shown). This latter observation also indicates that LPC incorporation into peptide-coupled liposomes does not lead to any significant quenching or dequenching of NBD-fluorescence per se. It must also be noted that for the lysoPC concentrations used in both assays, fusion competence could be fully restored upon removal of the inserted lyso compound by treatment with fatty-acid-free BSA. This indicates that the effects of LPC on fusion were not mediated by membrane solubilization and/or lysis.

Similar results were obtained when lysoPC was asymmetrically incorporated into vesicles during preparation (*30*) (outer-to-inner leaflet ratio 6.6:1), thus excluding potential artifacts arising from the presence of LPC micelles or soluble monomeric LPC, present in the bulk medium upon exogenous addition. The data, shown in Figure 7, indicate that although fusion is still present to a substantial extent (curve d), clustering is almost completely abolished (curve b). However, fusion was preceded by a lag time of ≈10 s and occurred to a limited extent as compared to fusion in the absence of LPC (compare curves c and d, and see below). These experiments indicate that high fusion levels can occur without any detectable oligomerization of the peptide molecules and point to the fact that peptide clustering is not a prerequisite for fusion.

b. Effect of Monoolein. Similar experiments as described above for lysophosphatidylcholine were performed with monoolein, which is known to facilitate negative spontaneous bilayer curvature and, in parallel, stalk formation and fusion (*29*). As shown in Figure 6, exogenous addition of monoolein resulted in an effective, dose-dependent promotion of fusion up to 350% (open squares), when compared to control levels. However, over the same concentration range, clustering of the peptide was affected to a far lesser extent than fusion (closed squares), suggesting that peptide oligomerization and fusion are not directly related.

Taken together, data presented in this and the previous paragraph indicate that, during peptide-induced fusion, peptide clustering may occur, which appears an accompanying event rather than a prerequisite for fusion. Differences in the kinetics of clustering cannot explain, therefore, the

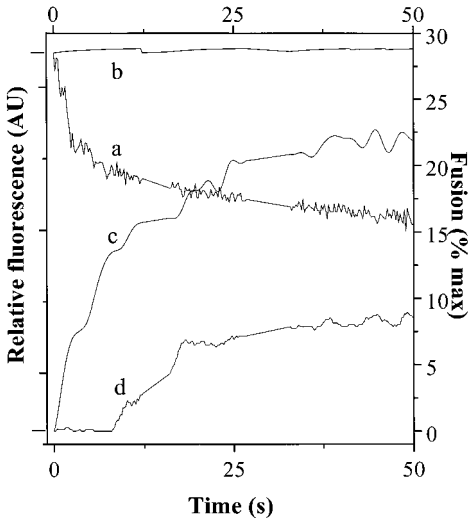

FIGURE 7: Effect of asymmetrically distributed lysoPC in the target membrane on WAE clustering and WAE-induced lipid mixing. DOPC-containing target liposomes were incubated for 5 min with 4% PEG 8000 (w/w), and then LPC was added from an aqueous stock solution to a final concentration of 2 mol %. After a 30 min incubation, liposomes were separated from PEG and LPC by gel filtration on a Sephadex G-25 column (PD-10, Pharmacia). These liposomes were then equilibrated at 37 °C in 10 mM Tris, 150 mM NaCl, pH 7.4, and WAE-coupled fluorescent liposomes were added (see legend to Figure 6). Clustering and fusion with liposomes devoid of LPC (a and c, respectively), and with LPC-containing liposomes (b and d, respectively), were monitored as described in Materials and Methods.

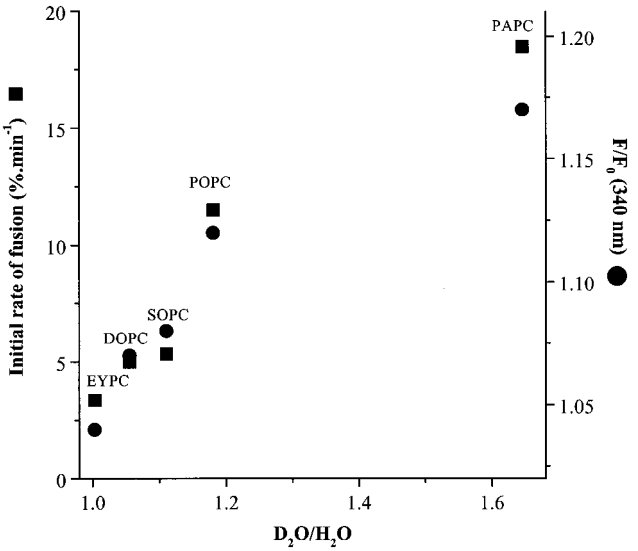

FIGURE 8: Effect of various PC species, present in the target membrane, on headgroup spacing, the initial rate of lipid mixing (left axis), and intrinsic Trp fluorescence (right axis). Liposomes of various PC species with 30 mol % cholesterol and containing 1 mol % dansylPE were equilibrated for 10 min at 30 °C; the fluorescence intensities in buffer made up in D_2O or H_2O were recorded, and the ratio D_2O/H_2O was calculated. The vesicles consisted of EYPC, DOPC, SOPC, POPC, or PAPC. All these measurements were performed in the absence of peptide vesicles. Headgroup spacing, thus assessed, was then plotted as a function of the initial fusion rate (■), determined after mixing of the various target vesicles and WAE-coupled vesicles. Details of the lipid mixing experiment are as described under Materials and Methods. To determine changes of intrinsic fluorescence of Trp (●), emission spectra (λ_{exc} = 280 nm) of WAE, coupled to liposomes, were recorded at 30 °C from 300 to 400 nm before and after addition of target vesicles of the indicated PC species composition. Samples were equilibrated for 3 min before measurement. The change in intrinsic fluorescence is expressed as F/F_0, where F and F_0 denote the fluorescence intensity at 340 nm after and before the addition of target vesicles, respectively. The lipid:peptide molar ratio was kept constant at 200 in all cases. Experiments were done in 10 mM Tris, 150 mM NaCl at pH 7.4. Error was within 5%.

PC lipid species dependence of WAE-induced fusion (Figures 1 and 4).

Bulk properties of the *target* membrane which presumably exert a level of control on membrane fusion include features such as lipid packing density, headgroup spacing, and degree of hydration. In the case of peptide-induced fusion, such features may affect the relative ease of the peptide to bind to the target membrane, to penetrate into its hydrophobic core, and to govern its ability to exhibit bilayer-to-nonbilayer transition. It is then plausible that differences in the fusion susceptibility among PC species might be related to subtle variations in those parameters. Some of these issues are addressed in the next sections.

Lipid Headgroup Spacing of the Target Membrane Modulates WAE-Induced Fusion. As proposed previously, on the basis of changes in intrinsic Trp fluorescence and its accessibility to quenching by iodide (*13*), shallow penetration into the target membrane is in all likelihood part of the mechanism of WAE-induced fusion. It becomes then conceivable that the *intrinsic* tightness of phospholipid headgroup interactions and, thus, headgroup spacing at the level of the target membrane (possibly governed by acyl chain unsaturation (*12*) and the presence of cholesterol (*32*)) could potentially influence the ease of penetration of the peptide into this target membrane. We therefore examined whether a relationship could exist between WAE-induced fusion and intrinsic headgroup spacing. To determine this, the fluorophore dansylPE was incorporated into target membranes of various lipid compositions, to assess hydration effects in the polar headgroup region as a measure of headgroup spacing (*21*). As shown in Figure 8, the headgroup hydration of various PC species (and thus headgroup spacing) increases according to a trend that accurately matches the influence of PC species on WAE-induced fusion (Figure 1): PAPC > POPC > SOPC > DOPC > EYPC. This indicates that the increase in fusion rates is *concomitant* to the increase in headgroup spacing. It is important to note that the size of the vesicles prepared of each lipid composition was similar (ca. 150 nm), excluding any artificial curvature effect.

Peptide Penetration into the Target Membrane Modulates WAE-Induced Fusion. A most appealing mechanism as to how headgroup spacing could modulate peptide-induced fusion would entail that spacing could facilitate the peptide's ability to penetrate into the target membrane. Although conclusive evidence as to a causal relationship between penetration and fusion is still lacking, the latter is thought to represent a crucial step in the overall mechanism of protein-induced fusion, e.g. in promoting negative bilayer, a condition facilitating membrane fusion (*3*, *25*, *31*, *38*; see also Discussion). Such an ability can be monitored as a function of the PC species composition of the target membranes, by following the changes in the intrinsic fluorescence of the Trp residue of the peptide. This fluorescence will increase when the amino acid senses a more hydrophobic environment, and in conjunction with an increase in quantum yield, the maximal spectral position will be shifted toward shorter wavelengths (blue shift). The

Table 1: Changes in Intrinsic Trp Fluorescence upon the Interaction of WAE-Coupled Vesicles with DOPC-Containing Target Vesicles as a Function of Temperature

temp (°C)	$\Delta\lambda_{max}$ (nm)[a]	F/F_0 (340 nm)[b]
10	red shift, 5 nm	0.75
15	red shift, 3 nm	0.89
20	0	1.005
25	7	1.05
30	8	1.07
37	8	1.15

[a] $\Delta\lambda_{max}$ indicates the shift of the emission maximum toward shorter wavelengths. Experimental conditions are as indicated in the legend to Figure 8. [b] See legend to Figure 8.

results, presented in Figure 8, demonstrate that the wider the intrinsic headgroup spacing of the PC species (at the level of target membranes), the more prominent the increase in fluorescence quantum yield (●). Hence, these data indicate that the migration of the Trp residue of WAE to a hydrophobic environment closely depends on the spacing of PC polar headgroups, i.e., that a wider headgroup spacing (thus a greater accessibility to the hydrophobic part of the target bilayer) promotes the ability of the peptide to engage in hydrophobic interactions with the target membranes, thereby facilitating the peptide-induced membrane destabilization leading to fusion.

Similarly, when such experiments as a function of temperature (Table 1) are carried out, it appears that the change in intrinsic Trp fluorescence closely parallels the extent of the shift in the emission maximum at a given temperature, both increasing when temperature increases. Hence, these data indicate that migration of the Trp residue to the hydrophobic region of the target bilayer is facilitated when temperature increases. This temperature-related ability of WAE to engage in hydrophobic interactions with target vesicles agrees well with iodide quenching data, as presented in Figure 9. Indeed, WAE becomes more shielded from the aqueous quencher when temperature increases, indicating that the temperature facilitates the peptide's interaction with the target membrane, presumably at the level of penetration.

Inclusion of LPC in the WAE fusion system, either exogenously added or incorporated into the outer leaflet of the target bilayer, exerted a dose-dependent impediment to the peptide's interaction with target membranes (Table 2), indicating that LPC reduces or even abolishes the peptide's capacity to engage in hydrophobic interactions with and to penetrate into the target membranes. This notion is supported by preliminary data obtained by Fourier transform infrared spectroscopy measurements (Pécheur, E. I., Martin, I., Ruysschaert, J. M., and Hoekstra, D., unpublished observations). When similar experiments were carried out in the presence of monoolein, changes observed in Trp fluorescence were comparable to those observed in the absence of monoolein (data not shown), suggesting that the fusion promotion by monoolein is not driven by facilitated peptide/lipid interactions or by increased peptide penetration into the target bilayer.

DISCUSSION

In the present work we have investigated the mechanism of membrane fusion induced by a membrane coupled peptide (WAE). Two issues in particular were addressed, i.e., peptide

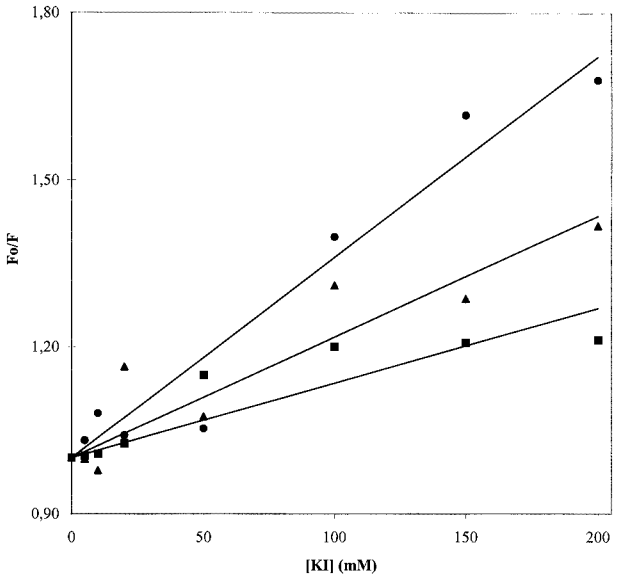

FIGURE 9: Stern−Volmer plots of Trp fluorescence quenching by I^- of peptide-coupled liposomes at various temperatures. WAE-coupled liposomes were preincubated for 1 min with DOPC-containing target vesicles, in a lipid:peptide molar ratio of 200. Trp fluorescence was measured before and after addition of increasing concentrations of KI. Results are expressed as F_0/F, where F_0 denotes the fluorescence intensity at 340 nm in the absence and F the fluorescence intensity in the presence of aqueous quencher, at 10 °C (●), 20 °C (▲,) and 37 °C (■). Error was within 4% at 10 °C and 6% at 20 and 37 °C.

Table 2. Changes in Intrinsic Trp Fluorescence upon the Interaction of WAE-Coupled Vesicles with DOPC-Containing Target Vesicles, in the Presence of LPC

[LPC] (μM)	$\Delta\lambda_{max}$ (nm)[a]	F/F_0 (340 nm)[b]
0	8	1.15
6, exogenous	red shift, 3 nm	0.93
12, exogenous	red shift, 5 nm	0.89
incorporated, outer leaflet	2 nm	1.04

[a,b] Same as footnotes to Table 1. Experiment was performed at 37 °C, after a 3 min preincubation of target vesicles in the presence of indicated concentrations of LPC.

clustering and the role of target membrane composition. The data reveal that, during the fusion process, clustering of the membrane-coupled peptide occurs. Evidence was obtained which suggests that clustering of WAE represents an accompanying event rather than a prerequisite for fusion.

Another novel feature of the present work is the remarkable dependence of peptide-induced fusion on lipid headgroup spacing in the target membrane. Experimental evidence suggests that such a parameter governs the relative ease of a coupled peptide to penetrate into the target membrane and subsequently engage in hydrophobic interactions, which presumably destabilizes the bilayer structure (*31*, *38*). Yet, the fact that PC species modulate such features is of special interest, particularly from a biological point of view, given that in previous studies PC has been merely considered to represent a hydration barrier to fusion. The present work suggests that one of its biological roles could well rely on conveying fusion-permissive properties to the fusion target site in a species-dependent manner.

Headgroup Spacing Regulates Peptide Penetration: Consequences for Fusion. Putative fusion domains of fusogenic viral proteins have been claimed to penetrate into target

membranes, thereby triggering the fusion event (*10, 11, 33*−*37*). As shown in the present work, modulating the peptide's accessibility to the hydrophobic core by varying headgroup spacing of the target membrane simultaneously modulates membrane fusion. Spacing between PC headgroups increases when shortening the *sn*-1 acyl chain (SOPC vs PAPC and POPC) and when increasing the degree of unsaturation of the *sn*-2 acyl chain (POPC and DOPC vs PAPC). Consistently, when headgroup spacing increases, an increase in intrinsic Trp fluorescence is seen (Figure 8), demonstrating that a wider headgroup spacing (and thus a potentially enhanced accessibility for the peptide to the hydrophobic part of the target bilayer) promotes the ability of the peptide to engage in hydrophobic interactions with the target membranes. Concomitantly, WAE-induced fusion increases (Figure 1 and Table 1), suggesting that both events are related. Previous evidence demonstrated (*13*) that the mechanism of WAE-induced fusion likely proceeds according to the stalk−pore mechanism. Formation of such a stalk is promoted by negative bilayer curvature (*31*), which acts as the driving force for membrane perturbation, pertinent to fusion. In the case of peptide-induced fusion, the relative ease of causing such a perturbation will likely depend on the ability of the peptide to engage in hydrophobic interactions and submerge into the bilayer/water interface. Although a variety of parameters may govern that ability, headgroup spacing will be an obvious one in this regard. Furthermore, peptides can induce either positive or negative curvature strain, depending on the distribution of their hydrophobic and hydrophilic residues (*38, 39*). Considering the narrow polar vs broad nonpolar helical face (hydrophobicity angle > 180°) (*13, 40, 41*), the ensuing wedgelike shape would readily explain the tendency of WAE to promote negative curvature strain (*25*).

In this regard, two important remarks must be made: First, anchorage of the peptide, thereby inducing geometrical constraints, plays a key role in conferring the proper conformation to WAE that allows its penetration into the target bilayer, namely an α-helical structure (*25*). Second, we demonstrated that the membrane-anchored WAE peptide analogue WAS, in which the Glu residues are randomly distributed in order to perturb the wedge shape, did not significantly penetrate into the target membrane (*25*). This indicates that the wedgelike structure of WAE may well represent a key regulating factor for WAE-induced fusion. Accordingly, the wider the headgroup spacing, the more easily the peptide will submerge, its wedgelike geometry forcing the lipids to tilt, thereby promoting negative bilayer strain (*39, 42*), stalk formation, and membrane merging, respectively.

Peptide Oligomerization Is Related to Peptide-Induced Fusion and Not Aggregation. Another novel feature revealed in the present work was the demonstration of peptide clustering or oligomerization, which exclusively occurs when fusion takes place and not upon vesicle aggregation, e.g. at temperatures below 10 °C, where aggregation occurs without fusion (Figures 1, 3, and 4). Indeed, the data indicate that, only upon clustering of WAE, PElys also becomes clustered; i.e., acceptor clustering appears to be driven by the ligand. WAE clustering is absent when fusion is abolished, while the degree of clustering increased when the rate of fusion increased (Figure 4). It thus appears that the rate of oligomerization is related to the kinetics of fusion. These features are very reminiscent of similar features reported for the behavior of fusogenic viral spike proteins (*43*−*47*). To our knowledge, the WAE model system provides the first demonstration that such a process occurs for a *membrane-anchored* peptide, emphasizing the relevance of this model to the study of (biological) membrane-bound protein-induced fusion.

The phenomenon of peptide clustering is thought to involve subtle peptide−peptide interactions, driven by α-helix/α-helix interactions through their hydrophobic face, as shown for several peptides (*41*) and proteins (*48*−*50*). This is likely also the case for WAE, which displays an amphipathic α-helical conformation when coupled to liposomes (*25*). However, spontaneous clustering of WAE on single vesicles does not occur. It would appear therefore that (an) additional factor(s) trigger(s) clustering, i.e., a factor that becomes operational only upon WAE's interaction with the target membrane at *fusogenic* conditions. This could suggest that the orientation of the peptide toward the target membrane could be a key regulating parameter in this respect.

A question directly related to this issue is then whether oligomerization represents a prerequisite for fusion. Our peptide-density-dependent experiments do not support this possibility, since a decrease in peptide density did not result in any significant delay in the onset of fusion (Figure 5). Such a delay has been observed in several viral model systems (*46, 47, 51*). In the latter systems such a lag phase has been interpreted in terms of conformational changes and/or rearrangements of fusion protein spikes into higher order oligomers, to form an "active" fusion complex. Although cooperativity in the formation of (viral) fusion protein aggregates has been questioned (*43*), the peptide-density-dependent experiments suggest that prior oligomerization of a fusogenic peptide is not an absolute prerequisite.

Further support for the absence of such a requirement was derived from experiments in which the effects of lysoPC and monoolein on fusion and clustering were examined. The results of these experiments revealed that the kinetics of fusion and clustering can be dissociated, in that they do not necessarily parallel each other. Of particular relevance are the lysoPC data (Figures 6 and 7 and Table 2). When lysoPC is incorporated into the target membrane, (i) peptide clustering is completely eliminated under conditions where fusion is still prominently occurring and (ii) measurements of changes of intrinsic Trp fluorescence revealed that the peptide penetration became significantly impaired (Table 2). Interestingly, further detailed studies have revealed that up to an exogenous concentration of 5 μM lysoPC, the decrease of intrinsic Trp fluorescence is commensurate with the decrease in the initial rate of fusion (Pécheur, E. I., Martin, I., Ruysschaert, J. M., and Hoekstra, D., unpublished observations). Although a correlation between penetration and fusion awaits further experimental support, these observations could suggest that a parameter related to the nature of the interaction of the peptide with the target membrane plays a key role in governing peptide clustering. This parameter may represent the hydrophobic interaction related to peptide penetration, which facilitates hydrophobic α-helix-driven peptide/peptide interactions as outlined above and which, accordingly, causes peptide clustering at the site of membrane

fusion. This course of events would be reminiscent to a scenario proposed by Danieli et al. (*43*), who suggest that penetration of one HA trimer, as a step in the mechanism of influenza virus fusion, may recruit neighboring, fusion peptide exposing trimers, thus giving rise to oligomerization of the HA complex.

Taken together, the present study demonstrates that peptide-induced fusion is regulated by the lipid composition of the target membrane. Such a regulation can be accomplished by variation in lipid headgroup spacing, which in turn governs the relative ease of penetration of the peptide into the bilayer, a step involved in the mechanism of protein-induced membrane fusion. Such peptide−lipid interactions can result in hydrophobic peptide−peptide interactions, causing peptide clustering. Our results suggest that peptide clustering is a consequence rather than a cause of peptide-induced membrane fusion. Finally, the results emphasize the validity of the WAE peptide to study the mechanism of membrane fusion in a biologically relevant context. Thus, the molecular and structural behavior of this membrane-anchored peptide may bear reminiscence to that of similarly membrane-associated peptides, located in viral proteins that bring about membrane fusion.

ACKNOWLEDGMENT

Dr. Leonid Chernomordik is gratefully acknowledged for suggestions regarding LPC experiments and helpful discussions.

REFERENCES

1. White, J. M. (1992) *Science 258*, 917−924.
2. Blobel, C. P., Wolfsberg, T. G., Turck, C. W., Myles, D. G., Primakoff, P., and White, J. M. (1992) *Nature 356*, 248−252.
3. Hoekstra, D. (1990) *J. Bioenerg. Biomemb. 22*, 121−155.
4. Phalen, T., and Kielian, M. (1991) *J. Cell. Biol. 112*, 615−623.
5. Asano, K., and Asano, A. (1988) *Biochemistry 27*, 1321−1329.
6. Yamada, S., and Ohnishi, S. I. (1986) *Biochemistry 25*, 3703−3708.
7. Vidal, M., and Hoekstra, D. (1995) *J. Biol. Chem. 270*, 17823−17829.
8. Moreau, P., Juguelin, H., Cassagne, C., and Morre, D. J. (1992) *FEBS Lett. 310*, 223−228.
9. Chernomordik, L. (1996) *Chem. Phys. Lipids 81*, 203-213.
10. Novick, S. L., and Hoekstra, D. (1988) *Proc. Natl. Acad. Sci. U.S.A. 85*, 7433−7437.
11. Harter, C., James, P., Bächi, T., Semenza, G., and Brunner, J. (1989) *J. Biol. Chem. 264*, 6459−6464.
12. Slater, S. J., Kelly, M. B., Taddeo, F. J., Ho, C., Rubin, E., and Stubbs, C. D. (1994) *J. Biol. Chem. 269*, 4866−4871.
13. Pécheur, E. I., Hoekstra, D., Sainte-Marie, J., Maurin, L., Bienvenüe, A., and Philippot, J. R. (1997) *Biochemistry 36*, 3773−3781.
14. Martin, F. J., Heath, T. D., and New, R. R. C. (1990) in *Liposomes: a practical approach.* (New, R. R. C., Ed.) pp 163−182, IRL Press, Oxford, U.K.
15. Puyal, C., Maurin, L., Miquel, G., Bienvenüe, A., and Philippot, J. (1994) *Biochim. Biophys. Acta 1195*, 259−266.
16. Cox, K. J., Ho, C., Lombardi, J. V., and Stubbs, C. D. (1992) *Biochemistry 31*, 1112−1117.
17. Klein, R. A. (1970) *Biochim. Biophys. Acta 210*, 486-489.
18. Bartlett, G. R. (1959) *J. Biol. Chem. 234*, 466−468.
19. Rudel, L. L., and Morris, M. D. (1973) *J. Lipid Res. 14*, 364−366.
20. Struck, D. K., Hoekstra, D., and Pagano, R. E. (1981) *Biochemistry 20*, 4093−4099.
21. Ho, C., S. J., S., and Stubbs, C. D. (1995) *Biochemistry 34*, 6188−6195.
22. Hoekstra, D. (1982) *Biochemistry 21*, 1055−1061.
23. Kok, J. W. and Hoekstra, D. (1993) in *Fluorescent and luminescent probes for biological activity. A practical guide to technology for quantitative real time analysis* Mason, W. T., Ed.) pp 100−119, Acad. Press, London.
24. Nichols, J. W., and Pagano, R. E. (1983) *J. Biol. Chem. 258*, 5368−5371.
25. Pécheur, E. I., Martin, I., Bienvenüe, A., Ruysschaert, J. M., and Hoekstra, D. (1998) *Biochemistry 37*, 2361−2371.
26. Smith, M., and Jungalwala, F. B. (1981) *J. Lipid Res. 22*, 697−704.
27. Hoekstra, D., Klappe, K., de Boer, T., and Wilschut, J. (1985) *Biochemistry 24* (18), 4739−4745.
28. Hoekstra, D., Klappe, K., Hoff, H., and Nir, S. (1989) *J. Biol. Chem. 264*, 6786−6792.
29. Lee, P. M., Cherry, R. J., and Bachi, T. (1983) *Virology 128*, 65−76.
30. Wu, H., Zheng, L. X., and Lentz, B. R. (1996) *Biochemistry 35*, 12602−12611.
31. Chernomordik, L., Kozlov, M. M., and Zimmerberg, J. (1995) *J. Membr. Biol. 146*, 1−14.
32. Ghosh, R. (1988) *Biochemistry 27*, 7750−7758.
33. Lear, J. D., and DeGrado, W. F. (1987) *J. Biol. Chem. 262*, 6500−6505.
34. Clague, M. J., Knutson, J. R., Blumenthal, R., and Herrmann, A. (1991) *Biochemistry 30*, 5491−5497.
35. Gray, C., Tatulian, S. A., Wharton, S. A., and Tamm, L. K. (1996) *Biophys. J. 70*, 2275−2286.
36. Rafalski, M., Ortiz, A., Rockwell, A., van Ginkel, L. C., Lear, J. D., DeGrado, W. F., and Wilschut, J. (1991) *Biochemistry 30*, 10211−10220.
37. Rapaport, D., and Shai, Y. (1994) *J. Biol. Chem. 269*, 15124−15131.
38. Epand, R. M., Shai, Y., Segrest, J. P., and Anantharamaiah, G. M. (1995) *Biopolymers 37*, 319−338.
39. Tytler, E. M., Segrest, J. P., Epand, R. M., Nie, S. Q., Epand, R. F., Mishra, V. K., Venkatachalapathi, Y. V., and Anantharamaiah, G. M. (1993) *J. Biol. Chem. 268*, 22112−22118.
40. Brasseur, R. (1991) *J. Biol. Chem. 266*, 16120−16127.
41. Kiyota, T., Lee, S., and Sugihara, G. (1996) *Biochemistry 35*, 13196−13204.
42. Horth, M., Lambrecht, B., Lay Khim, M. C., Bex, F., Thiriart, C., Ruysschaert, J. M., Burny, A., and Brasseur, R. (1991) *EMBO J. 10*, 2747−2755.
43. Danieli, T., Pelletier, S. L., Henis, Y. I., and White, J. M. (1996) *J. Cell. Biol. 133*, 559−569.
44. Freed, E. O., Delwart, E. L., Buchschacher, G. L. J., and Panganiban, A. T. (1992) *Proc. Natl Acad. Sci. U.S.A. 89*, 70−74.
45. Kielian, M., Klimjack, M. R., Ghosh, S., and Duffus, W. A. (1996) *J. Cell Biol. 134*, 863−872.
46. Bron, R., Wahlberg, J. M., Garoff, H., and Wilschut, J. (1993) *EMBO J. 12*, 693−701.
47. Clague, M. J., Schoch, C., and Blumenthal, R. (1991) *J. Virol. 1991*, 2402−2407.
48. McCoy, M., Stavridi, E. S., Waterman, J. L., Wieczorek, A. M., Opella, S. J., and Halazonetis, T. D. (1997) *EMBO J. 16* (20), 6230−6236.
49. Lemmon, M. A., Treutlein, H. R., Adams, P. D., Brunger, A. T., and Engelman, D. M. (1994) *Nat. Struct. Biol. 1* (3), 157−163.
50. Kleinschmidt, J. H., and Tamm, L. K. (1996) *Biochemistry 35*, 12993−13000.
51. Stegmann, T., Delfino, J. M., Richards, F. M., and Helenius, A. (1991) *J. Biol. Chem. 266*, 18404−18410.

BI981389U